0273-2289/00/84–86/1063/$14.00

Adsorption of Inulinases in Ion-Exchange Columns

F.-R. C. Silva and C. C. Santana*

School of Chemical Engineering, Universidade Estadual de Campinas, UNICAMP, CP 6066, CEP13083-970 Campinas, SP, Brazil, E-mail: santana@feq.unicamp.br

Abstract

The use of adsorption columns packed with ion-exchange resins for recovering, concentrating and purifying proteins is now widespread. The present work consists of a study on the dynamic behavior of adsorption columns that uses two kinds of adsorbents: a cationic and an anionic resin. A frontal analysis of the columns was performed with experimental data obtained from Fructozyme, a mixture of inulinase enzymes. The parameters of a Langmuir type of isotherm and adsorption kinetics were obtained from experimental tests in a batch system. A numerical technique based on orthogonal collocation and a fourth-order Runge-Kutta method was coupled with a nonlinear optimization method to predict the coefficients of the rate equations, which are fundamental for scale-up purposes.

Index Entries: Adsorption; enzyme adsorption; inulinases; ion-exchange; adsorption modeling.

Introduction

Inulin, a natural polymer formed by the linkage of fructose molecules, is a polyfructan. It is found in plants of the families *Compositae* and *Gramineae*. The monomers are united by β-2,1 linkages and the chain terminates with a glucose unit. The degree of polymerization of inulin depends on where and when the plant is grown. The average is about 30 U of fructose, which corresponds to a molecular weight of at least 5400, according to Vandamme and Derycke *(1)*. Inulinases are β-fructosidases, because they act exactly on and break the connections β-2,1 bord of the inulin. These enzymes are designated as 2,1-β-D-fructana-frutanohydrolases (EC 3.2.1.7). Besides being found in plants, inulinases can also be produced by mushrooms, bacteria, and yeasts. Two types of inulinases act in two ways. The enzymes that attack the glucosidic terminal of the inulin chain, breaking

*Author to whom all correspondence and reprint requests should be addressed.

Table 1
Properties of Inulinases as Related to the Producing Species

Mushroom	Mol wt (kDa)	Number	Reference
Aspergillus ficcum	64–66	3 endo 5 exo	*(2)*
Penicillium purpurogenum	64	1 endo	*(3)*
Aspergillus niger	53	1 endo 1 exo	*(4)*
Chysosporium pannorum	56–58	1 endo 1 exo	*(5)*

this chain continually in units of fructose, are called exoinulinases. Another form of attack is to break the glucosidic linkage in the center of the inulin chain so that the composition's degree of polymerization decreases by 2–5 U of fructose. These are called endoinulinasses, and their reaction products are fructose oligomers. The molecular masses of the endo- and exoinulinases are specific for each microorganism that produces them. Table 1 illustrates these differences.

As shown in Table 1, inulinases that contain more exoinulinases possess a larger molecular mass. Studies show that the range varies from 45 (smaller endoinulinase molecules) to almost 80 kDa (exoinulinase).

Materials and Methods

Materials

Fructozyme (a solution of crude material from *Aspergillus niger*) was a gift from Novo Nordisk (Araucaria, Brazil). This product contains endoinulinase and exoinulinase. Inulin from chicory was obtained from Fluka (Germany). The adsorbent CM-Sepharose CL-6B was obtained from Pharmacia; Accell Plus QMA was obtained from Waters. The column was series HR by Pharmacia. All other reagents were of analytical grade.

Determination of the Protein

Total protein content in solution was determined by the Lowry et al. *(6)* method using bovine serum albumin as standard.

Measurement of Enzymatic Activity

The enzymatic activity was measured by determining the concentration change of the reducing sugar via the Miller *(7)* method using fructose as standard. Enzymatic activity was measured by determining the amount of reducing sugar by incubating 200 μL of inulin solution (2% w/v) in 10 m*M* sodium acetate buffer, pH 4.1, and 30 m*M* Tris-HCl, pH 7.5, with 100 μL of enzyme solution, at 50°C for 10 min. One unit of inulinase is defined as the amount of enzyme producing 1 μmol of reducing sugar (expressed as g of fructose/min) under these standard conditions.

Mathematical Formulation: Finite Bath

A model that describes the enzyme adsorption on macroporous solids kinetics was presented by Carrére *(8)* and Horstmann and Chase *(9)*. This model was adopted in the present work and includes the mass transfer in the particle liquid film, the diffusion in the particle's adsorbent pores, and the surface adsorption rate. The main reason for using this model was to obtain phenomenological parameters that are coefficients in the adsorption equations, by using simple experiments such as the finite bath. The optimized parameters were obtained by coupling kinetic experimental data to the set of equations and optimization methods based on least square methods. This procedure can be used for scale-up processes, in either batch or column adsorption. The model equations follow.

Mass balance over a solid particle correspond to the differential equation that describes the solute (enzyme) diffusion in the particle's adsorbent pores:

$$\varepsilon_p \frac{\partial C_i}{\partial t} = \varepsilon_p D_{ef} \left(\frac{\partial^2 C_i}{\partial r^2} + \frac{2}{r} \frac{\partial C_i}{\partial r} \right) - \frac{\partial q_i}{\partial t} \tag{1}$$

in which ε_p = the porosity of the particle; C_i = the enzyme concentration in the liquid phase in the interior of the particle's pores; q_i = the enzyme concentration in the particles; D_{ef} = the effective diffusion coefficient; t = the temporal variable; r = spatial (radial) variable *(3)*.

The initial and boundary conditions are as follows:

$$t = 0 \quad C_i = 0 \quad \forall r \tag{2}$$

In the particle's center,

$$r = 0 \quad \frac{\partial C_i}{\partial_r} = 0 \tag{3}$$

On the surface,

$$r = R \quad \varepsilon_p D_{ef} \frac{\partial C_i}{\partial_r} = k_f \left(C_b - C_i \mid_{r=R} \right) \tag{4}$$

in which R = the particle's radius; and k_f = the external mass transfer convective coefficient.

According to Eq. 4, the mass transfer rate through the liquid film is related to the global concentration of protein in the liquid phase C_b and to the concentration of enzyme in the liquid phase of the particle's pores $C_i \mid r = R$.

Adsorption kinetics on the pores' surface are expressed by

$$\frac{\partial q_i}{\partial_t} = k_1 C_i \left(q_m - q_i \right) - k_2 q_i \tag{5}$$

in which k_1 = the adsorption kinetics constant; k_2 = the desorption kinetics constant; q_m = the maximum adsorbed quantity; and q_i = the quantity adsorbed in a time interval t.

Considering a very fast adsorption rate on the surface, an equilibrium ($\partial q_i/\partial t = 0$) can be reached such that Eq. 5 can be written as follows:

$$q_i = [q_m C_i/(k_d + C_i)] \tag{6}$$

in which $k_d = k_2/k_1$.

With this simplification, Eq. 1 becomes

$$\varepsilon_p \frac{\partial C_i}{\partial t} = \varepsilon_p D_{ef}\left(\frac{\partial^2 C_i}{\partial r^2} + \frac{2}{r}\frac{\partial C_i}{\partial r}\right) - \frac{q_m k_d}{(k_d + C_i)^2}\frac{\partial q_i}{\partial t} \tag{7}$$

Mass balance in the liquid phase with global enzyme concentration (batch mode) is calculated as follows:

$$\frac{dC_b}{dt} = -\frac{3vk_f}{\varepsilon_p R V_l}(C_b - C_i) \tag{8}$$

in which v = the adsorbent volume; and V_l = the liquid volume.

The initial condition for Eq. 8 is

$$t = 0 \quad C_b = C_0 \tag{9}$$

in which C_0 = the initial liquid-phase enzyme concentration.

Defining the following dimensionless groups,

$$x = \frac{r}{R} \quad \Theta_i = \frac{C_i}{C_0} \quad \Theta_b = \frac{C_b}{C_0} \quad \tau = \frac{tD_{ef}}{R^2} \quad B_{im} = \frac{k_f R}{\varepsilon_p D_{ef}} \tag{10}$$

(when applied to the previous equations) gives the following results:

Mass balance over a solid particle:

$$\left[1 + \frac{q_m k_d}{\varepsilon_p (k_d + C_0\Theta_i)^2}\right]\frac{\partial \Theta_i}{\partial \tau} = \left(\frac{\partial^2 \Theta_i}{\partial x^2} + \frac{2}{x}\frac{\partial \Theta_i}{\partial x}\right) \tag{11}$$

$$\tau = 0 \quad \Theta_i = 0 \quad \forall x \tag{12}$$

$$x = 0 \quad \frac{\partial \Theta_i}{\partial x} = 0 \tag{13}$$

$$x = 1 \quad \frac{\partial \Theta_i}{\partial x} = B_{im}(\Theta_b - \Theta_i|_{x=1}) \tag{14}$$

Mass balance in the liquid phase:

$$\frac{d\Theta_b}{d\tau} = -\frac{3v}{V_l} B_{im} (\Theta_b - \Theta_i |_{x=1}) \tag{15}$$

$$\tau = 0 \quad \Theta_b = 1 \tag{16}$$

When the variable transformation $u = x^2$ is applied to Eqs. 11 and 14, and the spatial variable is discretized through the orthogonal collocation method as proposed by Finlayson *(10)*, Villadsen and Michelsen *(11)*, and Yao and Tien *(12)*, we have:

$$\left[1 + \frac{q_m k_d}{\varepsilon_p (k_d + C_0 \Theta_{ij})^2}\right] \frac{d\Theta_{ij}}{d\tau} = 4u_j \sum_{k=1}^{N+1} B_{jk} \Theta_{ik} + 6 \sum_{k=1}^{N+1} A_{jk} \Theta_{ik} \quad (j = 1 \ldots N) \tag{17}$$

$$\tau = 0 \quad \Theta_{ik} = 0 \quad k = 1 \ldots N+1 \tag{18}$$

$$x = 1 \quad \sum_{k=1}^{N+1} A_{N+1,\,k} \Theta_{ik} = \frac{B_{im}}{2} (\Theta_b - \Theta_{iN+1} |_{x=1}) \tag{19}$$

The collocation points are N interior $0 < u < 1$ and one boundary point $u_{N+1} = 1$. The point $u = 0$ is not included because the symmetry condition requires that the first derivative be 0 at $u = 0$, and that condition is built into the trial function.

The ordinary differential Eqs. 15 and 17, together with the respective initial conditions, Eqs. 16, 18, and 19, form an ordinary differential equation system that can be integrated by known methods such as the fourth-order Runge-Kutta method.

Experiments in Agitated Tanks

The experimental method in agitated tanks consists of using a shaker bath to keep the adsorbate-adsorbent mixture homogeneous and at constant temperature. This method provides a continuously agitated enzyme solution with a given initial concentration of adsorbate in contact with the adsorbent. The solution concentration was followed until the samples, which were analyzed in a spectrophotometer, were withdrawn. In this work, the system was monitored in two ways: by the protein assay following the Lowry *(6)* method, and by the analysis of reduced sugars as described by Miller *(7)*. Adsorption capacity of the adsorbent can be determined by analyzing the kinetics curves and through equilibrium tests that indicate values of the equilibrium concentration.

The systems studied were the CM-Sepharose CL-6B and Accell Plus QMA resin with Fructozyme. Each experiment was done with a given initial concentration of the protein solution. The experimental apparatus

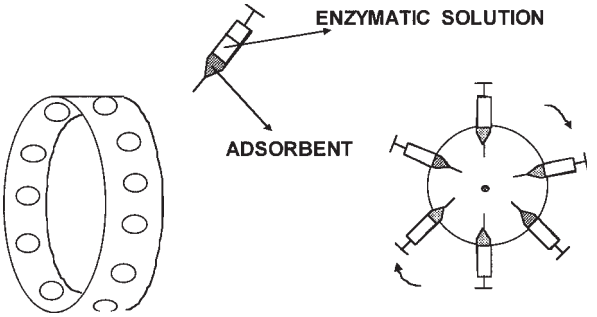

Fig. 1. Experimental scheme used in the experiments in a batch adsorption.

consisted of a 1-mL syringe containing the solution of interest; an ultraviolet (UV) monitor for absorbance reading at 750 and 540 nm, respectively; and assay protein and sugars reduced analysis. Figure 1 shows the experimental setup that used these components.

Mathematical Formulation: Lumped Model in Packed Column

Because most adsorption in concentration and separation practice is in packed columns, an adsorption column must be modeled for analysis of parameters as well as scale-up procedures. A mathematical formulation, based mainly on Carrére's *(8)* work, is thus established as follows:

The mass balance in a column for single-component adsorption, including axial dispersion and rate flow constant is described by:

$$\varepsilon_b \frac{\partial C_e}{\partial t} = D_a \frac{\partial^2 C_e}{\partial z^2} - v_s \frac{\partial C_e}{\partial z} - \frac{3}{R} K_1 (1 - \varepsilon_b)\,(C_e - C_i)_{r=R} \tag{20}$$

Equation 20 can be solved by using the boundary conditions of Danckwertz:

$$v_s C_o = v_s C_e \big|_{z=0} - D_a \frac{\partial C_e}{\partial z}\big|_{z=0} \tag{21}$$

$$\frac{\partial C_e}{\partial z}\big|_{z=Z} = 0 \quad t > 0 \tag{22}$$

and initial conditions:

$$t = 0 \quad \forall z \quad C_e = 0 \tag{23}$$

To obtain the dimensionless form of Eq. 20 and boundary conditions of Eqs. 21 and 23, the following change of variables is proposed:

$$\tau = \frac{t v_s}{Z},\ Pe = \frac{Z v_s}{D_a},\ v_s = \frac{V_s}{\varepsilon_b},\ y = \frac{z}{Z}, \text{ and } \lambda = \frac{3K_1}{R}\,\frac{Z}{v}\left(\frac{1-\varepsilon_b}{\varepsilon_b}\right)$$

With these definitions, the mass balance equation and the boundary and initial conditions can be presented as follows:

$$\frac{\partial C_e}{\partial \tau} = \frac{1}{Pe}\,\frac{\partial^2 C_e}{\partial y^2} - \frac{\partial C_e}{\partial y} - \lambda\,(C_e|_y - C_i|_{r=R}) \tag{24}$$

$$v_s C_o = v_s C_e|_{y=0} - \frac{1}{Pe}\,\frac{\partial C_e}{\partial y}|_{y=0} \tag{25}$$

$$\frac{\partial C_e}{\partial y}|_{y=1} = 0 \quad \tau > 0 \tag{26}$$

$$\tau = 0 \quad \forall z \quad C_e = 0 \tag{27}$$

The numerical difficulties associated with solving the differential equations system formed by Eqs. 13 and 24 can be avoided by simplifying the model related to diffusion in pores (Eq. 13), which lumps the parameters involved in mass transfer. In this way the dependence of the internal concentration C_i with the particle radii r is disregarded, being C_i substituted by an average concentration $\overline{C}_i(t)$, defined by

$$\overline{C}_i(t) = \frac{1}{V_p}\int v_p C_i(r, t)\, dV_p \tag{28}$$

Applying the average volume operator to the particle diffusion model gives:

$$\varepsilon_p \frac{d\overline{C}_i}{dt} = \frac{3}{R}\,K_1\,(C_e - \overline{C}_i) - \frac{dq_i}{dt} \tag{29}$$

in which

$$\frac{dq_i}{dt} = f'(\overline{C}_i)\,\frac{d\overline{C}_i}{dt} \tag{30}$$

$$f(\overline{C}_i) = \frac{q_m \cdot k_d}{(k_d + \overline{C}_i)} \tag{31}$$

The initial condition can be applied as

$$t = 0 \quad \overline{C}_i = 0 \tag{32}$$

In Eq. 29 the mass transfer coefficient, K_1, is defined as

$$1/K_1 = [(1/k_e) + (1/\varepsilon_p k_i)] \tag{33}$$

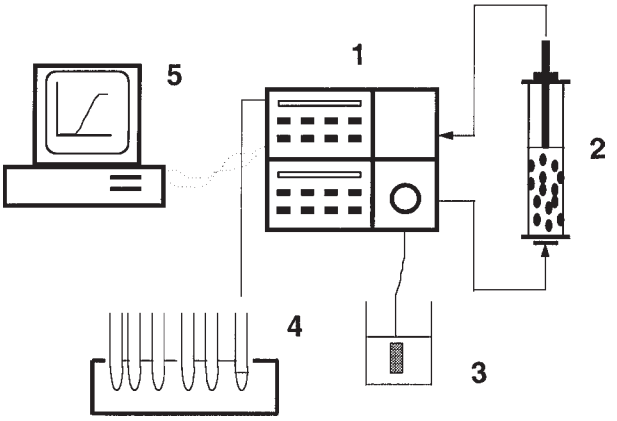

Fig. 2. Experimental setup for columns runs: (1) piston pumps and UV detector; (2) fixed-bed column; (3) enzyme solution; (4) fraction collector; and (5) data-acquisition system.

in which K_e = the mass transfer coefficient in the external (pores) liquid phase; and K_i = the mass transfer coefficients in the internal (pores) liquid phase.

In obtaining the global model, two approaches were introduced. The first was for the kinetics of adsorption:

$$\frac{1}{V_p}\int v_p \frac{f'(C_i)}{dC_i}\frac{\partial C_i}{\partial t}\,dV_p \cong \frac{f'(\bar{C}_i)}{d\bar{C}_i}\frac{d\bar{C}_i}{\partial t} \tag{34}$$

and the second was the evaluation of the overall mass transfer coefficient, K_l. In particular, on the right-hand side of Eq. 33 the local mass transfer coefficient K_i appears:

$$K_i = D_{ef}(\partial C_i/\partial r)\,|_{r=R}\,(C_e - \bar{C}_i) \tag{35}$$

The exact value of K_i is a function of time and can be evaluated only through the complete model.

Experiments in Packed Column

The experimental devices used for the adsorption studies are detailed in Fig. 2. A glass column (0.5 cm diameter and 8 cm long) was used for the packed-bed experiments. This system was equilibrated with 10 m*M* sodium acetate, pH 4.1, and 30 m*M* Tris-HCl, pH 7.5, in CM-Sepharose CL-6B and Accel Plus QMA resins, respectively. The breakthrough curve was obtained after the saturation capacity in the packed bed was reached, the monitoring was done with a UV-visible detector, and samples were collected and analyzed later. The bed porosity for the adsorbents CM-Sepharose CL-6B and Accel Plus QMA was characterized by the tracer pulse method of

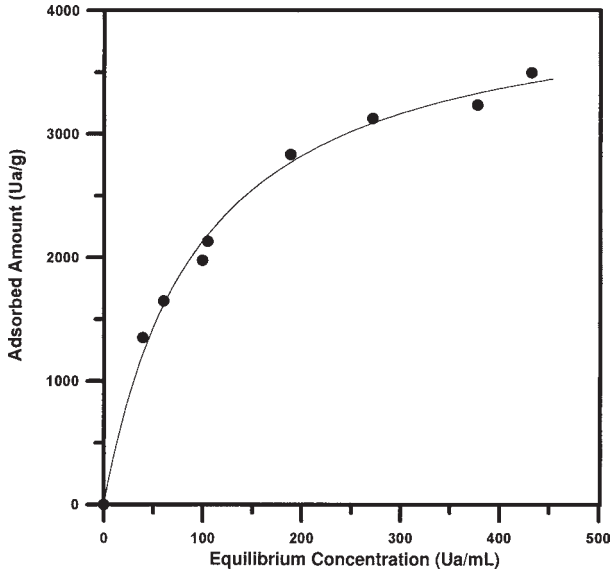

Fig. 3. Isotherm fitted by the Langmuir model for the system Fructozyme-CM Sepharose CL-6B. $q = 4165.59\ C/(94.80 + C)$.

Arnold et al. *(13)*. The values of bed porosities were 0.60 and 0.47, and particle porosities were 0.41 and 0.59, respectively.

Results and Discussion

The study of the adsorption of the inulinase in CM-Sepharose CL-6B and Accel Plus QMA resins was accomplished through solid-liquid equilibrium. Buffers used were 10 m*M* sodium acetate (pH 4.1) and 30 m*M* Tris-HCl (pH 7.5), respectively, with experiments performed in 1-mL syringe tubes, containing the enzymatic solution, as described previously. The system was under constant agitation and the controlled temperature reached equilibrium after 4 h. The obtained isotherms in terms of enzyme activity followed a Langmuir model, as shown in Figs. 3 and 4. Values of q_m and k_d for the adsorbent CM-Sepharose CL-6B and Accell Plus QMA for the Fructozyme extract are expressed in activity units and are depicted in Figs. 3 and 4.

The study of the kinetics of adsorption was accomplished with the objective of identifying the adjusted diffusion coefficient and convective mass transfer coefficient for the two pairs of adsorbent-adsorbate, as pointed out in the mathematical formulation objectives. Figures 5–7 show the kinetics curves. Table 2 shows the optimized values for the parameters D_{ef} and k_f, as obtained from the nonlinear optimization method, proposed by Box *(14)*, for the cationic adsorbent CM-Sepharose CL-6B. These results show that for this system, the parameter k_f remains almost constant for a threefold dilution whereas the parameter D_{ef} increases almost four times

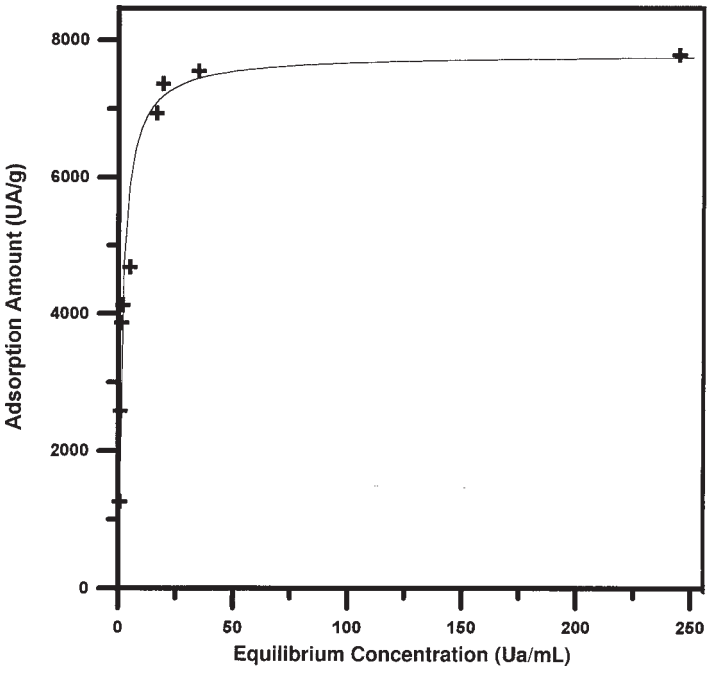

Fig. 4. Isotherm fitted by the Langmuir model for the system Fructozyme-Accell Plus QMA. $q = 7783.25\ C/(1.611 + C)$.

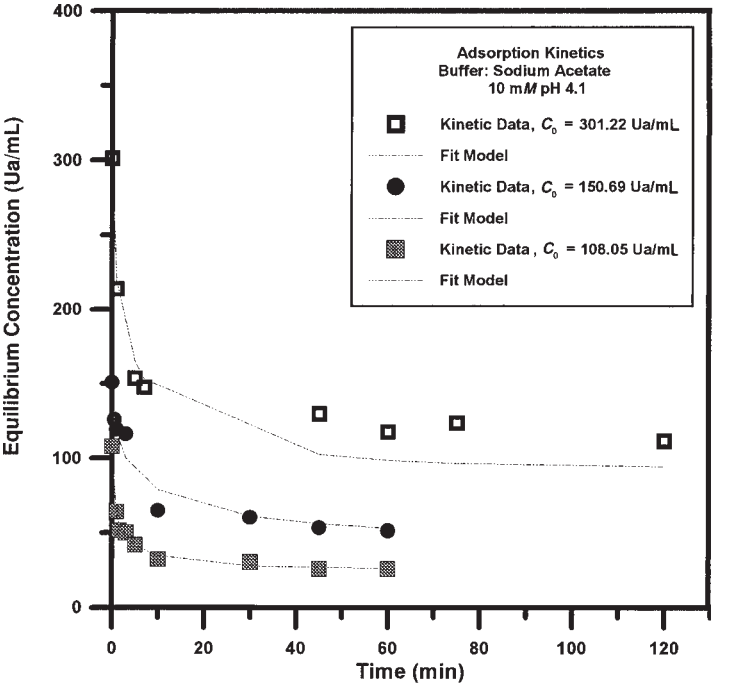

Fig. 5. Kinetic curves fitted by the mathematical model for the system Fructozyme-CM Sepharose CL-6B.

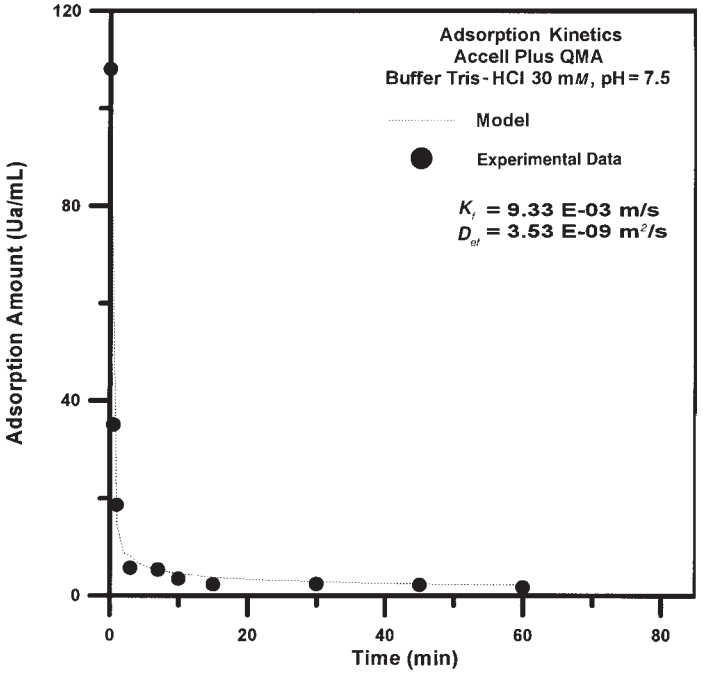

Fig. 6. Kinetic curves fitted by the mathematical model for the system Fructozyme-Accell Plus QMA (low-capacity level).

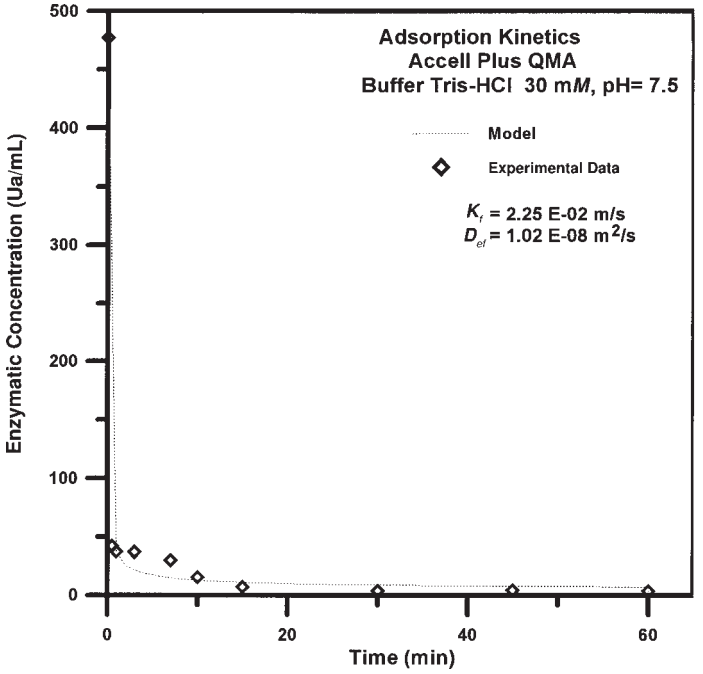

Fig. 7. Kinetic curves fitted by the mathematical model for the system Fructozyme-Accell Plus QMA (high-capacity level).

Table 2
Optimized Parameters for Batch Experiments with Fructozyme-CM-Sepharose CL-6B System

Inulinase concentration (Ua/mL)	$K_f \times 10^4$ (m/s)	$D_{ef} \times 10^{11}$ (m^2/s)
301.22	1.38	1.10
150.69	1.65	3.70
108.05	1.72	4.43

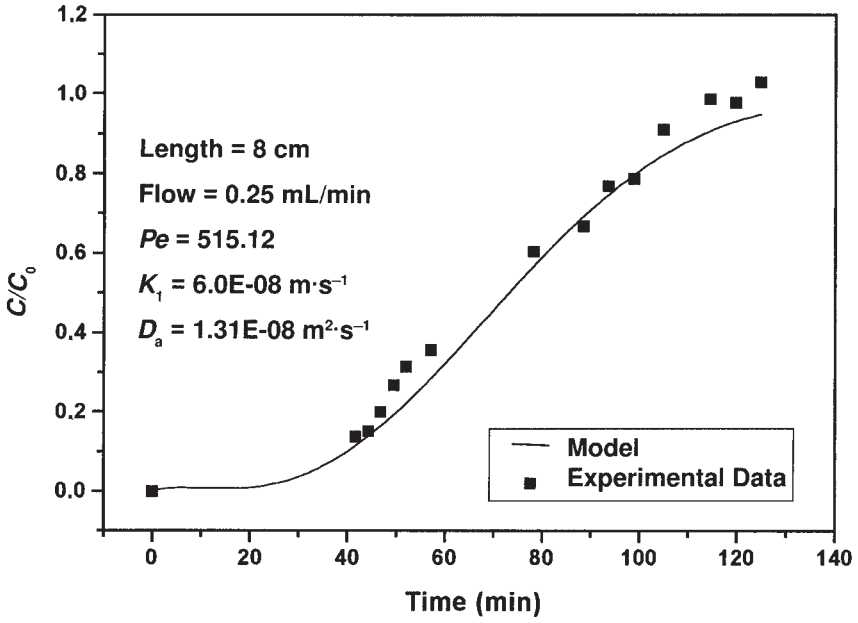

Fig. 8. Breakthrough curve and column model adjustment for the system Fructozyme-CM Sepharose CL-6B (flow rate = 0.25 mL/min).

for the same dilution range. Considering the anionic adsorbent Accel Plus QMA, the adjusted parameter k_f decreased approximately an order of magnitude as concentration decreased fourfold, whereas; D_{ef} decreased approximately threefold for the same concentration range.

To complete the column dynamic study, breakthrough curves for the adsorption of Fructozyme in the adsorbents CM-Sepharose CL-6B and Accell Plus QMA were obtained experimentally. Figures 8–10 depict the experimental curves adjusted by the mathematical model presented earlier to describe column dynamics. Curve adjustment shows that the model describes the column dynamics in the adsorption of Fructozyme in both systems quite well.

To demonstrate the concentration effect for a cycle of adsorption/elution, an elution curve after washing the column with the buffer and eluting

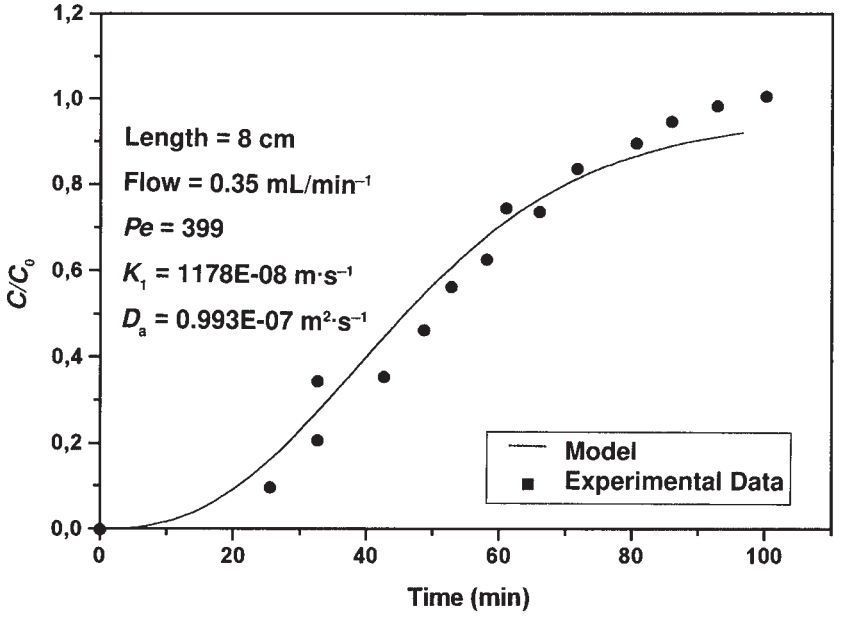

Fig. 9. Breakthrough curve and column model adjustment for the system Fructozyme-CM Sepharose CL-6B (flow rate = 0.35 mL/min).

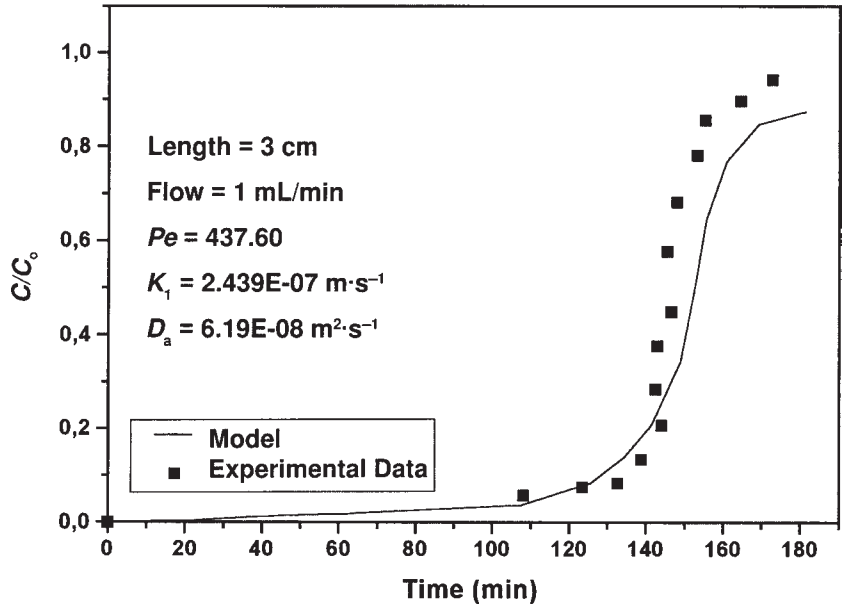

Fig. 10. Breakthrough curve and column model adjustment for the system Fructozyme-Accell Plus QMA.

with a 0.5 *M* NaCl solution is presented in Fig. 11. Recovery of enzyme expressed in activity was 70%, and an increase in activity in terms of UA/milliliter reached 13 times the initial activity.

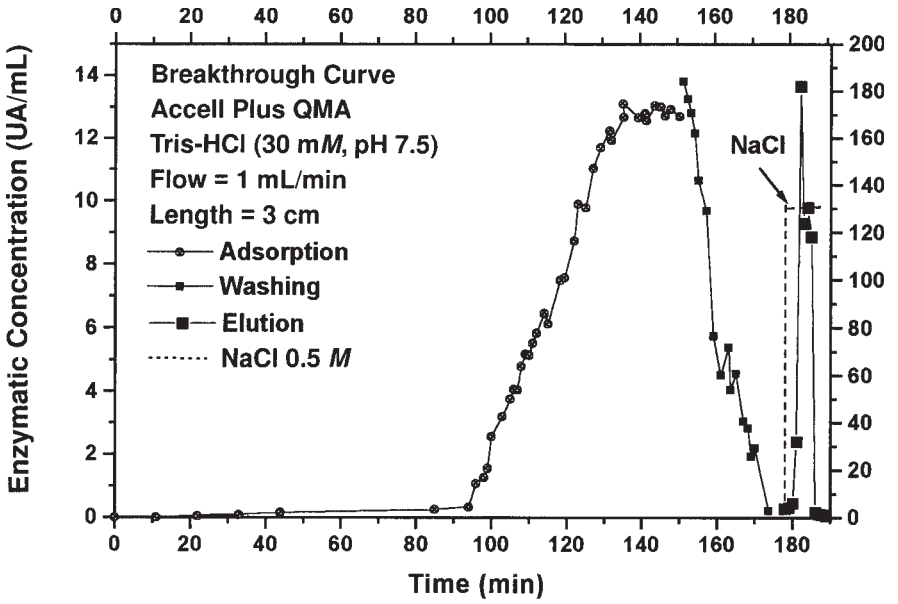

Fig. 11. Elution curve for Fructozyme after washing with 0.5 *M* NaCl solution.

Conclusion

The study of the behavior of the inulinase enzymes in ion-exchange adsorption systems was shown to be useful for the quantitation of the adsorption procedure, because the ion-exchange step is normally included in any purification process as a concentration step. The adsorption isotherm obeys a Langmuir-type model for the adsorbents used (CM-Sepharose CL-6B and Accel Plus QMA resins). A mathematical model, based on data obtained with agitated tanks, allowed the determination of mass transfer parameters for use in scale-up of the process. Breakthrough curves for several operational conditions, as well as an elution curve to reach a concentration factor of 13 in the activity of the Fructozyme extract in a cycle of adsorption/elution, were obtained for the adsorbent Accel Plus QMA. Recovery of the enzyme reached 70% for the adsorption/elution cycle.

Acknowledgments

We are grateful to CAPES, Brazil, for the scholarship to F.R.C.S. and to Novo Nordisk for the supply of the enzymatic extracts.

Appendix: Nomenclature

A = matrix of orthogonal collocation
B = matrix of orthogonal collocation
B_{im} = Biot number
C_b = liquid-phase enzyme concentration (mg · cm^{-3})

C_b = external enzyme concentration (mg · cm^{-3})
C_i = particle pore enzyme concentration (mg · cm^{-3})
$\overline{C}_i(t)$ = average enzyme concentration (mg · cm^{-3})
C_o = initial bulk liquid-phase enzyme concentration (mg · cm^{-3})
c^* = equilibrium concentration (mg · cm^{-3})
D_a = axial dispersion
D_{ef} = effective diffusion coefficient (m^2 · min^{-1})
K_L = global mass transfer coefficient (m · min^{-1})
k_d = dissociation constant (mg · cm^{-3})
k_f = external mass transfer convective coefficient (m · min^{-1})
k_i = internal mass transfer coefficient (m · min^{-1})
k_1 = adsorption kinetic constant (cm^3 · mg^{-1} · min)
k_2 = desorption kinetic constant (cm^3 · mg^{-1} · min)
N = orthogonal collocation points number
Pe = Peclet number
q^* = equilibrium concentration (mg · g^{-1})
q_i = solid-phase enzyme concentration (mg · g^{-1})
q_m = maximal capacity of the solid phase (mg · g^{-1})
R = particle radius (m)
r = spatial (radial) variable (m)
t = temporal (time) variable (min)
u = dimensionless spatial variable
V_1 = liquid-phase volume (cm^3)
v = solid-phase volume (cm^3)
v_s = superficial velocity (m · s^{-1})
v_s = interfacial velocity (m · s^{-1})
x = dimensionless spatial variable
y = dimensionless spatial variable
Z = dimensionless spatial variable
z = length (m)
ε_b = bed porosity
ε_p = particle porosity
τ = dimensionless spatial variable
θ = dimensionless concentration
$_b$ = index, refers to bulk liquid phase
i = index, refers to pore liquid phase
j = index, refers to orthogonal collocation point ($j = 1 \ldots N$)
k = index, refers to orthogonal collocation point ($k = 1 \ldots N + 1$)

References

1. Vandamme, E. J. and Derycke, D. G. (1983), *Adv. Appl. Microbiol.* **29,** 139–176.
2. Ettalibi, M. and Baratti, J. C. (1990), *Agric. Biol. Chem.* **54,** 61–68.
3. Onodera, S. and Shiomi, N. (1988), *Agric. Biol. Chem.* **52(10),** 2569–257.
4. Azhari, R., Szlak, A. M., Ilan, E., Sideman, S., and Lotan, N. (1989), *Biotechnol. Appl. Biochem.* **11,** 105–117.
5. Xiao, R., Tanida, M., and Takao, S. (1989), *J. Ferment. Bioengineering* **67,** 244–248.

6. Lowry, O. H., Rosebrough, N. J., Farr, A. L., and Randall, R. J. (1951), *J. Biol. Chem.* **193,** 265–275.
7. Miller, G. L. (1959), *Anal. Chem.* **31,** 426–428.
8. Carrére, H. (1993), PhD thesis, Institut National Polytechnique de Toulouse, Toulouse, France.
9. Horstmann, B. J. and Chase, H. A. (1989), *Chem. Eng. Res. Dev.* **67(3),** 243–254.
10. Finlayson, B. A. (1980), *Nonlinear Analysis in Chemical Engineering*, 2nd ed., McGraw-Hill, New York.
11. Villadsen, J. E. and Michelsen, M. L. (1978), *Solution of Differential Equation Models by Polynomial Approximation*, 3rd ed., Prentice-Hall, NJ.
12. Yao, C. and Tien, C. (1992), *Chem. Eng. Sci.* **47(2),** 465–473.
13. Arnold, F. H., Blanch, H. W., and Wilke, C. R. (1985), *Chem. Eng. J.* **30,** B25–B36.
14. Box, P. (1965), *Computer J.* **8,** 42–52.